

Available online at [www.sciencedirect.com](http://www.sciencedirect.com)

ScienceDirect

journal homepage: <http://www.elsevier.com/locate/rpor>

## Original research article

# An improved neutron autoradiography set-up for $^{10}\text{B}$ concentration measurements in biological samples



Ian Postuma<sup>a,b,\*</sup>, Silva Bortolussi<sup>a,b</sup>, Nicoletta Protti<sup>a,b</sup>,  
 Francesca Ballarini<sup>a,b</sup>, Piero Bruschi<sup>a</sup>, Laura Ciani<sup>c</sup>, Sandra Ristori<sup>c</sup>,  
 Luigi Panza<sup>d</sup>, Cinzia Ferrari<sup>e</sup>, Laura Cansolino<sup>e</sup>, Saverio Altieri<sup>a,b</sup>

<sup>a</sup> Department of Physics, University of Pavia, Italy<sup>b</sup> National Institute of Nuclear Physics, INFN, Section of Pavia, Italy<sup>c</sup> Department of Chemistry 'UgoSchi' & CSGI, University of Florence, Florence, Italy<sup>d</sup> DISCAFF, University of Eastern Piedmont, Novara, Italy<sup>e</sup> Dipartimento di Scienze Clinico-Chirurgiche, Diagnostiche e Pediatriche, Università degli Studi di Pavia, Italy

## ARTICLE INFO

## Article history:

Received 18 March 2014

Received in revised form

28 May 2015

Accepted 21 October 2015

Available online 14 November 2015

## Keywords:

Boron Neutron Capture Therapy

Boron concentration

Neutron autoradiography

CR-39

## ABSTRACT

**Aim:** Boron Neutron Capture Therapy (BNCT) is a binary hadrontherapy which exploits the neutron capture reaction in boron, together with a selective uptake of boronated substances by the neoplastic tissue. There is increasing evidence that future improvements in clinical BNCT will be triggered by the discovery of new boronated compounds, with higher selectivity for the tumor with respect to clinically used sodium borocaptate (BSH) and boronophenylalanine (BPA).

**Background:** Therefore, a  $^{10}\text{B}$  quantification technique for biological samples is needed in order to evaluate the performance of new boronated formulations.

**Materials and methods:** This article describes an improved neutron autoradiography set-up employing radiation sensitive films where the latent tracks are made visible by proper etching conditions.

**Results:** Calibration curves for both liquid and tissue samples were obtained.

**Conclusions:** The obtained calibration curves were adopted to set-up a mechanism to point out boron concentration in the whole sample.

© 2015 Greater Poland Cancer Centre. Published by Elsevier Sp. z o.o. All rights reserved.

## 1. Background

Boron Neutron Capture Therapy (BNCT) is a binary hadrontherapy consisting in the administration of a boronated

compound like boronophenylalanine (BPA), which concentrates more  $^{10}\text{B}$  in tumor than in healthy tissue. After boron administration the tumor site is irradiated with low energy neutrons, causing neutron capture reactions in boron. This nuclear interaction releases two high LET particles (an alpha

\* Corresponding author at: Dip. Fisica, Università di Pavia, via Bassi 6, 27100 Pavia, Italy. Tel.: +39 0382 987635.

E-mail addresses: [ian.postuma@pv.infn.it](mailto:ian.postuma@pv.infn.it) (I. Postuma), [silva.bortolussi@pv.infn.it](mailto:silva.bortolussi@pv.infn.it) (S. Bortolussi).

<http://dx.doi.org/10.1016/j.rpor.2015.10.006>

1507-1367/© 2015 Greater Poland Cancer Centre. Published by Elsevier Sp. z o.o. All rights reserved.

particle and a lithium ion) that deposit all their energy inside the cell. BNCT can thus deliver a therapeutic dose to the tumor while sparing the healthy tissue, triggering and possibly achieving tumor control.

The development of new  $^{10}\text{B}$  delivery systems, with higher selectivity for the tumor with respect to clinically used sodium borocaptate (BSH) and boronophenylalanine (BPA) will trigger future improvements in clinical outcomes of Boron Neutron Capture Therapy.<sup>1</sup> A  $^{10}\text{B}$  concentration measuring technique for biological samples is needed in order to evaluate the performance of new boronated formulations. At the Triga Mark II nuclear reactor in Pavia, two techniques were developed: Alpha Spectrometry (AS)<sup>2</sup> and Quantitative Neutron Capture Radiography (QNCR).<sup>3</sup> The latter was recently improved to ensure higher accuracy and optimized efficiency when a high number of samples is analyzed.

In the first QNCR set-up, described by Gadan et al.,<sup>3</sup> a suitable calibration curve and a sufficient resolution were achieved; however, there was still potential for improvements. Firstly, it was necessary to reduce the time of the overall procedure, determined by an etching time longer than 2 h. This would increase the time efficiency of the set-up and possibly open the road to quasi-online blood borne boron concentration measurements. Secondly, in order to reduce the background signal, a better selection of the tracks left on the Solid State Nuclear Track Detector<sup>b</sup> (SSNTD) by  $^7\text{Li}$  and  $\alpha$  particles had to be achieved. The latter condition would simplify data acquisition, avoiding the implementation of a complex morphological track selection algorithm that was previously necessary to reject the tracks due to protons.<sup>c</sup> Furthermore, this would improve the resolution of the measurement. These goals were reached employing PEW40 ( $\text{KOH} + \text{C}_2\text{H}_5\text{OH} + \text{H}_2\text{O}$ ) as a chemically etching solution at  $70^\circ\text{C}$ , instead of the NaOH solution previously used. This set-up decreased the etching time from 2 h to 10 min. Moreover, only tracks from  $^7\text{Li}$  and  $\alpha$  ions are thus detected, decreasing by consequence the relative error of the calibration from 7% at  $1\sigma$  of C.L. to 5% at  $1\sigma$  of C.L.

## 2. Aim

To further exploit the features of autoradiography, another QNCR technique was set up to perform a quantitative imaging of the  $^{10}\text{B}$  distribution in a biological tissue sample.<sup>5</sup> These images can then be compared to histological preparation of contiguous sections in order to have a proof that  $^{10}\text{B}$  concentrates in the tumor with respect to the normal tissue. This quantitative imaging was attained by merging adjacent pictures throughout a scan of the area where the sample was fixed on the SSNTD. The tracks of each image were then analyzed with the QNCR set-up reported in Section 2.4. Consequently it was possible to reassemble the image of the whole sample outlining the  $^{10}\text{B}$  concentration distribution.

The QNCR set-up was then validated by comparing the outcome of boron concentration measurements of the same

sample with alpha-spectrometry (AS) results.<sup>2</sup> Moreover, through a collaboration with a group working at the Comision Nacional de Energia Atomica (CNEA, Argentina), tissue and cell samples treated with BPA (following a routine administration protocol) were measured by QNCR and AS in Pavia and by ICP-AES, ICP-MS and QNCR with different films in Buenos Aires. Although the project is in an early stage, results show that all the cited techniques are consistent for  $^{10}\text{B}$  concentration measurements.

This improved neutron autoradiography method was then applied to  $^{10}\text{B}$  concentration measurements in tissues from small animals and cell cultures treated with new carriers, within the framework of the BNCT feasibility study for osteosarcoma.<sup>6</sup> The experiments were carried out testing three categories of carriers: gold nano-particles, liposomes, polymeric nano-particles and BPA as a reference. In particular,  $^{10}\text{B}$  loaded liposomes and BPA were administered to Sprague-Dawley rats bearing osteosarcoma. After treatment, healthy muscle and tumor mass were explanted and prepared for QNCR and AS. The results concerning boron biodistribution obtained in these tissues are presented and discussed here. Boron biodistribution obtained *in vivo* will be used in the following part of the experiment, consisting in *in vivo* irradiation of rats with osteosarcoma to test BNCT efficacy in tumor remission and BNCT toxicity for healthy tissues.

## 3. Material and methods

CR-39<sup>d</sup> was used as SSNTD, as described in Gadan et al.,<sup>3</sup> thus, before proceeding with boron concentration measurements, the bulk etch rate associated with the new etching method was characterized as a comparison to the previous set-up. Subsequently the most favorable irradiation conditions were chosen. Calibration curves were then built both for liquids and tissue samples. These results were then used for boron concentration measurements of tissue samples from animals administered with different boronated substances. The same samples were then analyzed with the AS method,<sup>2,6</sup> thus validating this new QNCR set-up.

Subsequently, the calibration curves were employed to develop a c++ program in the ROOT<sup>7</sup> framework to recombine the microscopic images resulting from a scan of the whole irradiated tissue sample. The output of the software was a macroscopic boron concentration map.

### 3.1. Bulk etch rate measurement

To characterize the track formation in a SSNTD, as extensively described in 3, the first step consists in the evaluation of the bulk etch rate  $V_b$ .

$V_b$  was measured and compared to the one obtained by Gadan et al.,<sup>3</sup> thus highlighting the differences of the etching conditions in the two setups. For  $V_b$  measurement, the CR-39 films were etched for the following times: 0, 2, 4, 8, 10, 20, 30 and 60 min, in a PEW40 solution at  $70^\circ\text{C}$ , which was obtained

<sup>b</sup> These kinds of detectors were recently used to display boron at cellular level [4].

<sup>c</sup> In biological tissues protons with an energy of 590 keV are produced by the neutron capture reaction on nitrogen:  $^{14}\text{N}(\text{n},\text{p})^{14}\text{C}$ .

<sup>d</sup> Rectangular polyallyldiglycol carbonate (PADC), from Intercast Europe manufacturer, with  $75\text{ mm} \times 25\text{ mm}$  area and 1 mm width.

by mixing: 15% of KOH, 40% of  $C_2HeO$  and 45% of pure water; where % represents the mass per cent. After each etching time the thickness of the SSNTD was measured employing a Mitutoyo device (LITEMATIC VL-50AS, with a sensitivity of  $0.1 \mu m$ ) in 20 randomly chosen points. The mean values of thickness and the standard deviation were then calculated, plotted and analyzed by means of a routine in ROOT framework.

### 3.2. Calibration samples preparation and irradiation

For boron measurement by neutron autoradiography, a calibration curve expressing the track density as a function of boron concentration must be assessed. The first step was to perform measurements using tissue and liquid standards with known boron concentration in order to obtain two calibration curves, expressed as density of tracks [tracks/ $mm^2$ ] versus boron concentration in ppm. Standard liquid and tissue samples with known boron concentration are used as reference.

The liquid standards consisted of water solutions of  $^{10}B$  at 5, 10, 25, 50 and 100 ppm. About 1 ml of each solution was poured on CR-39 films, using the device constructed for the purpose the irradiation of liquid samples that allows irradiating 4 films at a time with 4 samples each.<sup>3</sup> This device was irradiated at the end of the thermal column of the TRIGA Mark II reactor, operating at 20 kW for 30 min, receiving a neutron fluence of  $(10.4 \pm 0.4) \times 10^{10} N/cm^2$ . After irradiation, CR-39 films were chemically etched for 10 min with the same etching parameters used for the bulk etch rate calculations.

The tissue standards were obtained from a mixture of liver cells and a solution of BPA fructose in different fixed proportions<sup>3</sup> to obtain reference concentrations of 10, 19, 43, 57 and 75 ppm ( $\mu g/g$ ). These samples were frozen in small cylindrical rods at  $-80^\circ C$ . Afterwards,  $60 \mu m$  thick sections were obtained using a Leica cryostat and were deposited on CR-39 films, that were then irradiated at the end of the thermal column with the reactor operating at 2 kW for 30 min receiving a neutron fluence of  $(1.97 \pm 0.01) \times 10^{10} N/cm^2$ . After irradiation, films were chemically etched with described etching conditions for 10 min.

Another parameter that must be taken into account for tissue calibration is the amount of water loss occurring after the preparation of the tissue sections. This is necessary since distinct tissues may lose water in different percentages; therefore, the dry to fresh mass ratio is needed to renormalize the result with respect to the calibration curve. To measure the mass loss due to evaporation, the same set-up as in 3 was used.

### 3.3. Track density analysis

After the irradiation and etching (see result in Fig. 1), the procedure consisted of 3 further steps: image acquisition, image analysis and data analysis. The experimental set up for the Image acquisition is composed by a microscope<sup>e</sup> connected to a lamp<sup>f</sup> and a joystick.<sup>g</sup> The microscope has an integrated

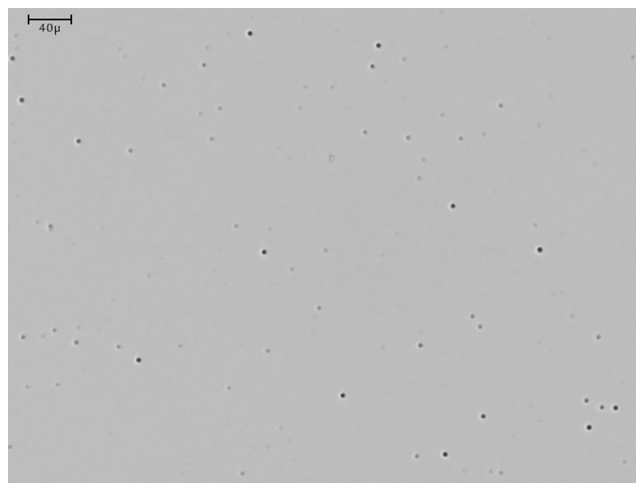


**Fig. 1 – Microscopic image of an irradiated and etched SSNTD of a tissue standard with 10 ppm of boron.**

camera connected to a PC and images are acquired and analyzed with Image Pro Plus 7.0.<sup>8</sup> Once the acquisition process is concluded, Image Pro Plus allows to perform some operations in the picture. The first one is the background subtraction to eliminate the inhomogeneities. Subsequently, the contrast of the picture is enhanced, in a way to increase the visibility of the tracks left by the particles. The contrast enhancement is performed keeping the same parameters for all the analyzed pictures, since the acquisition conditions are the same.

The last phase of image analysis consists in selecting and counting<sup>h</sup> the tracks, according to the gray scale.<sup>i</sup> For the purpose of the analysis, only dark objects are selected, the range of the selected gray scale is fixed for all the analyzed pictures. Finally, before counting the tracks, the interesting morphological parameters of the dark objects are selected: the ratio of the radii<sup>j</sup> of the tracks and their area. The first one is important since it is an estimator of track roundness; if the value is near 1 then the track has a circular shape, at increasing ratios the track becomes less circular. The latter parameter depends on the ionizing particle energy.<sup>9</sup> From each analyzed picture, a file is created reporting these parameters for each analyzed track.

These files are then analyzed with a ROOT program. The data analysis starts by imposing a threshold to reject objects with radius less than 2 pixels and radius ratio greater than 1.6 to remove artifacts or film defects from the counting mechanism. Non perpendicular tracks and overlapping tracks can be neglected since the etching time and neutron irradiation were accurately selected. Moreover, Fig. 2 shows that tracks, from the boron neutron capture reaction have a circular shape and a well defined area. Therefore, it is easy to separate physical tracks from artifacts or superimposed tracks. Subsequently, the remaining tracks are counted yielding the density of tracks

<sup>h</sup> Count/Size function of Image Pro.

<sup>i</sup> The light set-up is repeatable, the lamp is fixed at a certain luminosity output and the effect of surrounding light is negligible.

<sup>j</sup> The radii ratio is the ratio between the maximum and minimum distance from the border to the center of the track.

<sup>e</sup> LEICA MZ16A.

<sup>f</sup> LEICA CLS150X.

<sup>g</sup> PRIOR OPTISCAN II.

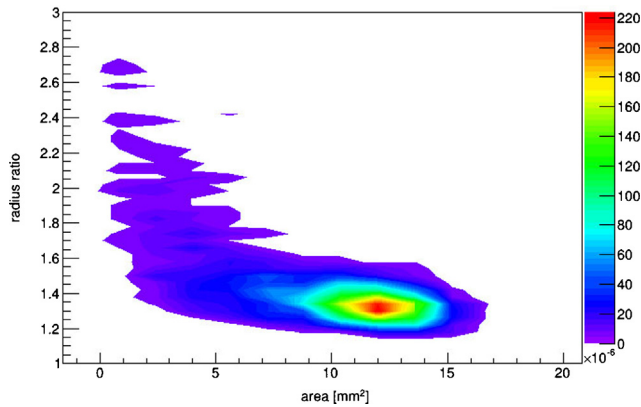


**Fig. 2 – Scatter plot showing the relation between the track area and the radius ratio.**

in one picture. The identical method is applied to each analyzed random microscopic picture of the same sample. These data are then converted in an histogram plotting the distribution of the track density per picture. The histogram follows a normal distribution, that is then fitted with a Gaussian, giving the mean track density and the associated standard deviation. Finally, the track density is divided by the area of a picture<sup>k</sup> in  $\text{mm}^2$ .

### 3.4. Boron distribution analysis

Once the calibration curves were obtained, it was possible to use them to measure boron concentration in samples treated with boronated substances. Instead of randomly taking picture through the sample area, a uniform scan in a predetermined area<sup>l</sup> ( $\approx 1 \text{ cm}^2$ ) was implemented. This picture sampling was possible because Image Pro Plus can manage the movable table that is installed in the Leica microscope. Again, as in Section 2.3, the software outputs files recording the track morphological characteristics.

These files were analyzed with a home made c++ software that makes use of ROOT functionalities. Accordingly, threshold values were imposed, then for each picture the track density was calculated. Thus, by comparison with the tissue calibration curve, for each picture the boron concentration was evaluated by taking into account water evaporation. Finally, these values were plotted in a 3D histogram where each color represents a  $^{10}\text{B}$  concentration value, resulting in a map of boron concentration.

For this analysis, two sections of the same sample were taken. The first  $60 \mu\text{m}$  thick slice was deposited on the SSNTD for the quantitative analysis. While the second adjacent slice of  $10 \mu\text{m}$  was deposited on a microscope slide which was then stained with hematoxylin and eosin. This enabled the comparison of the boron distribution map with a histological image,

<sup>k</sup> The picture has an area of  $0.2961 \text{ mm}^2$ , each picture has  $5\text{Mp}$  resolution corresponding to  $2739 \times 1826$  pixels.

<sup>l</sup> The selection of the area depends on the dimensions of the analyzed sample.

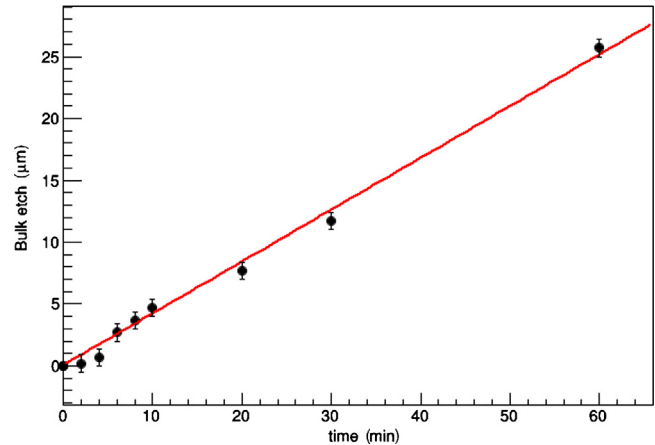


**Fig. 3 – Amount of material removed (bulk etched) as a function of time. The fit was performed with a linear equation and the fluctuations are a consequence of the error of the measurement.**

allowing an immediate evaluation of the selectivity in boron absorption by the tumor nodules.

## 4. Results

### 4.1. Bulk etch rate

The thickness of the removed layer as a function of the etching time, measured as described in Section 2.1, is shown in Fig. 3. Etching increases linearly in time with a bulk etch rate of  $V_b = (25.1 \pm 0.6) \mu\text{m/h}$ . This is 15 times faster than the previous etching conditions.<sup>3</sup>

### 4.2. Calibration for the liquid sample

The calibration curve for the liquid sample is shown in Fig. 4, the fit results linear with a slope of  $0.112 \pm 0.006 \text{ ppm mm}^2/\text{tracks}$ . There is no visible saturation effect and values are expressed with  $1\sigma$  confidence level.

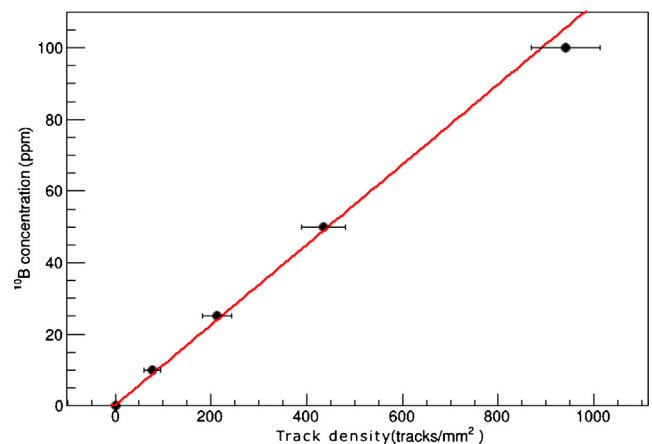


**Fig. 4 – Calibration curve for liquid samples; boron concentration as a function of track density. The fit has been performed with a linear equation.**

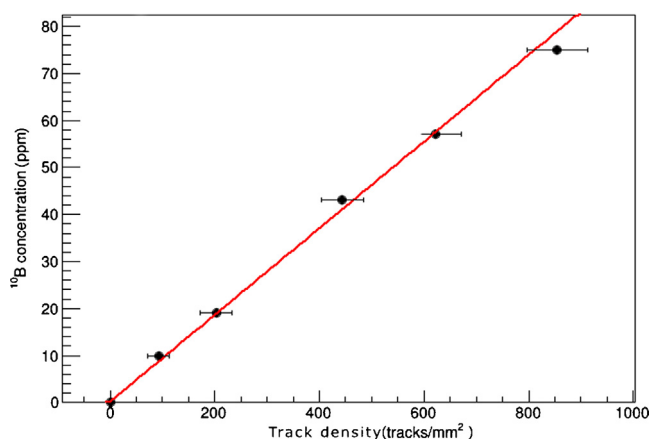


**Fig. 5 – Tissue calibration curve; boron concentration as a function of track density. The fit has been performed with a linear equation.**

The limit of boron detection (LOD) is  $\approx 0.5$  ppm while the limit of quantification (LOQ) is  $\approx 1.5$  ppm. Therefore, this set-up can be reliably used to measure boron concentrations from 1.5 to 100 ppm, which is the usual range found in a clinical BNCT.

#### 4.3. Calibration for the tissue sample

The calibration curve for the tissue sample is shown in Fig. 5, again the fit results linear with a slope of  $0.092 \pm 0.004$  ppm mm<sup>2</sup>/tracks. As stated in Section 2.2 the dry to fresh mass ratio was measured, for the reference tissue sample this value corresponds to  $0.17 \pm 0.01$ . There is no visible saturation effect and values are expressed with  $1\sigma$  confidence level. The LOD is  $\approx 0.5$  ppm while the LOQ is  $\approx 1.5$  ppm. Therefore, this set-up can be reliably used to measure boron concentrations from 1.5 to 100 ppm, which is the usual range found in a clinical BNCT.

#### 4.4. Boron concentration map

This technique was applied on tissue samples of Sprague-Dawley rats bearing osteosarcoma and administered with BPA. The result of the analysis is shown in Fig. 6a. From the comparison with the histological image (Fig. 6b) of the same sample, it is evident that boron concentrates more in the cancerous mass than in the healthy tissue. Moreover, the ratio between boron

concentration in the tumor with respect to the normal tissue ( $\approx 3.5$ ) resulted very similar to the value found in literature, in other tumors treated with BPA.<sup>10</sup>

## 5. Conclusions

The calibration curves obtained for both liquid and solid samples are very precise and the linearity in the whole range of concentrations tested is excellent, thus they can be employed for boron concentration measurements in BNCT studies. More precisely this set-up was, and will be, adopted for the research of new boronated compounds such as: <sup>10</sup>B loaded liposomes, gold nano particles and polymeric nano particles. Results obtained in these works are described in 11,6.

Comparing the new set-up with 3 some improvements were achieved. At first, the etching time was reduced from  $\approx 2$  h to 10 min: this dramatically increases the efficiency of the method because it speeds up the sample preparation before the microscopic analysis. Moreover, there is no evidence of proton contamination, from neutron capture reaction in nitrogen. Since the track density in tissue samples without boron is almost 0 and the tracks detected in such samples come only from protons generated by neutron capture in nitrogen. Therefore, the results with control samples demonstrate that this method is not sensitive to protons. This simplifies the image analysis, since there is no need to morphologically separate the tracks generated by protons from the tracks generated by a particles or lithium ions. The only trigger is the constraint on radius and radius ratio to remove signals originated from artifacts or film defects. In fact, the calibration accuracy, which is determined by the relative error of the calibration slopes, was reduced from 6% to 4%. Another aspect that has changed with respect to the former protocol is the fact that the track density is now lower. As a consequence, it was possible to calibrate the system for a wider range of <sup>10</sup>B concentrations.

Finally, as shown in Section 3.4, it was possible to employ the tissue calibration curve for quantitative boron distribution measurements. This increases the possible applications of neutron autoradiography in BNCT, in fact it is a useful method to have deeper insights into boron biodistribution in tumor and different healthy tissues. As demonstrated by dedicated studies performed by the Argentinean BNCT group, in order to obtain a successful BNCT treatment, it is essential that boron is taken up uniformly by tumor.<sup>12</sup> Thus, it is important to quantify boron concentration in terms of tumor to normal

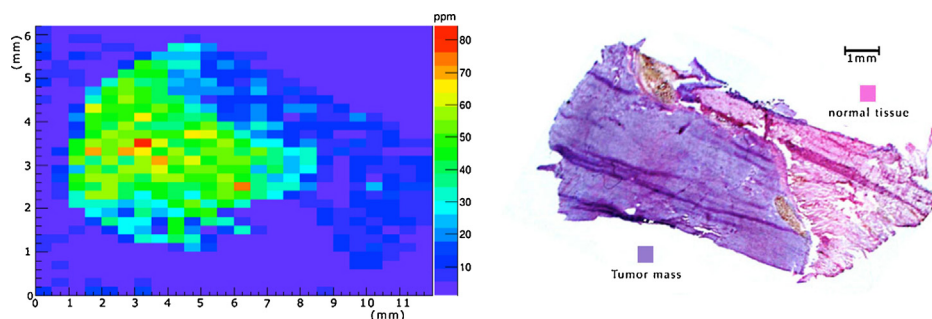


**Fig. 6 – Comparison of (a) <sup>10</sup>B distribution in a tissue sample of a Sprague-Dawley rat bearing osteosarcoma with the corresponding (b) histological image of a subsequent slice of the tissue sample.**

tissue ratio, but also to investigate carefully the homogeneity of boron distribution inside tumor. Neutron autoradiography allows this kind of analysis with high precision at the tissutal level. Therefore, autoradiography might be an actor in increasing knowledge on the correlation between boron distribution and BNCT outcome, thanks to its ability to quantify the micro distribution of boron in tumor and healthy tissues.

---

### Conflict of interest

None declared.

---

### Financial disclosure

None declared.

### REFERENCES

---

1. Barth RF. A critical assessment of boron neutron capture therapy: an overview. *J Neurooncol* 2003;**62**:111–21.
2. Bortolussi S, Altieri S. Boron concentration measurement in biological tissues by charged particles spectrometry. *Radiat Environ Biophys* 2013;**52**:493–503.
3. Gadan MA, Bortolussi S, Postuma I, et al. Set-up and calibration of a method to measure  $^{10}\text{B}$  concentration in biological samples by neutron autoradiography. *Nucl Instrum Methods* 2012:51–6.
4. Portu AM, Rossini AE, Gadan MA, et al. Experimental set up for the irradiation of biological samples and nuclear track detectors with UV C. *Rep Pract Oncol Radiother* 2014;**11**.
5. Altieri S, Bortolussi S, Bruschi P, et al. Neutron autoradiography imaging of selective boron uptake in human metastatic tumours. *Appl Radiat Isotopes* 2008;**66**(12):1850–5.
6. Bortolussi S, Ciani L, Postuma I, et al. Boron concentration measurements by alpha spectrometry and quantitative neutron autoradiography in cells and tissues treated with different boronated formulations and administration protocols. *Appl Radiat Isotopes* 2013;**88**:78–80.
7. Brun R, Rademakers F. Root – an object oriented data analysis framework. Proceedings AIHENP'96 workshop. *Nucl Inst Methods Phys Res* 1997. See also <http://.root.cern.ch/1>.
8. Image-pro plus software. Silver Springs, MD: Media Cybernetics.
9. Nikezic D, Yu KN. Formation and growth of tracks in nuclear track materials. *Mater Sci Eng* 2004;**46**:51–123.
10. Barth RF, Coderre JA, Vincente MGH, Blue TE. Boron neutron capture therapy of cancer: current status and future prospects. *Clin Cancer Res* 2005;**11**:3987–4002.
11. Ciani L, Bortolussi S, Postuma I, et al. Rational design of gold nanoparticles functionalized with carboranes for application in boron neutron capture therapy. *Int J Pharm* 2013;**458**:340–6.
12. Molinari AJ, Thorp SI, Portu AM, et al. Assessing advantages of sequential boron neutron capture therapy (BNCT) in an oral cancer model with normalized blood vessels. *Acta Oncol* 2014:1–8. PMID: 24960584.